Journal of Applied Polymer Science

Preparation and Characterization of Extruded Nanocomposite Based on Polycarbonate/Butadiene-Acrylonitrile-Styrene Blend Filled with Multiwalled Carbon Nanotubes

Wegrzyn Marcin,[1] Adolfo Benedito,[1] Enrique Gimenez[2]

[1]Departamento de Materiales, Instituto Tecnológico del Plástico (AIMPLAS), Calle Gustave Eiffel 4, 46980 Paterna, Spain
[2]Instituto de Tecnología de Materiales, Universidad Politécnica de Valencia, Camino de Vera, 46022 Valencia, Spain
Correspondence to: W. Marcin (E-mail: marcinwegrzyn@hotmail.com)

ABSTRACT: Nanocomposites of polycarbonate/acrylonitrile-butadiene-styrene (PC/ABS) with multiwall carbon nanotubes (MWCNT) prepared by masterbatch dilution are investigated in this work. Melt compounding with twin screw extruder is followed by complete characterization of morphology, rheological-, mechanical-, and thermal-properties of the nanocomposites. Light-transmission- and scanning electron microscopy shows the preferential location of MWCNT in the PC. Nevertheless, relatively good dispersion in the whole matrix is achieved, what is corroborated with the specific mechanical energy. The study of viscoelastic properties of PC/ABS-MWCNT shows the fluid–solid transition below 0.5 wt % MWCNT. Beyond this point the continuous nanofiller network is formed in the matrix promoting the reinforcement. Addition of 0.5 wt % MWCNT reduces ductility of PC/ABS and enhances Young's modulus by about 30% and yield stress by about 20%. Moreover, theoretical values of stiffness calculated within this work agree with the experimental data. Electrical conductivity, showing percolation at 2.0 wt % MWCNT, are influenced by processing temperature. © 2013 Wiley Periodicals, Inc. J. Appl. Polym. Sci. **2014**, *131*, 40271.

KEYWORDS: blends; nanotubes; graphene and fullerenes; mechanical properties; theory and modeling; extrusion

Received 23 August 2013; accepted 8 December 2013
DOI: 10.1002/app.40271

INTRODUCTION

Miscible- and multiphase-polymer blends create over 36% of the polymer production industry.[1] The development of nanocomposites based on a matrix filled with multiwalled carbon nanotubes (MWCNT) offers novel possibilities in the production of materials with tailored properties. Both miscible[2] and immiscible[3,4] blends exhibit desired performance characteristics after the incorporation of MWCNT. Carbon nanotubes characterized by a unique structure and uncommon properties have already reached an important position in science and technology. High aspect ratio causes the boost of electrical and thermal conductivity of insulating polymers at relatively low loads.[5,6] Likewise, the shape and properties of MWCNT allow for the improvement of mechanical properties of the polymer matrix when homogeneous dispersion is achieved. This is related to the mechanical percolation based on interactions between carbon nanotubes and polymer chains.[7] Nevertheless, achieving a good dispersion of carbon nanotubes in polymers by melt-mixing is a key challenge. The agglomeration level based on attractive Van der Waals forces between individual nanotubes appears to be tunable when twin-screw extrusion is applied.[8] Tailoring the key processing parameters during nanocomposite preparation and further processing[9] allows for a significant decrease of agglomeration and control of alignment in the final part.[10] Specific mechanical energy (SME) is a recognized parameter describing the energy applied to the material during melt-mixing.[11] Proper control of the compounding process and selection of correct processing parameters (in particular, the design of the screw profile), are significant factors in the quality of the final nanocomposite.[8] There are some examples in the literature of melt-mixed nanocomposites of carbon nanotubes in commodity polymers, such as polyethylene,[12] polypropylene,[13] and polystyrene.[14] Materials based on engineering plastics such as polycarbonate (PC) have attracted considerable interest in recent years. Alig et al.[15] reported strong relation between electrical conductivity, MWCNT content and processing parameters for nanocomposites based on PC. The destruction of the nanofiller network and thus, a decrease in electrical conductivity, was reported when high screw speed was used. Primary- and secondary agglomeration theory explains that nanofiller bundling is related to electrical conductivity reinforcement in plastics.[6] Presence of tightly packed agglomerates in the nanofiller before extrusion makes deagglomeration more difficult, decreasing the

homogeneity of MWCNT dispersion. However, it is claimed that the size of carbon macro-structures can be modified by changing the shear conditions, for example, with ball mill treatment of nanotubes before further processing.[16] Proper parameters (high screw speed and low barrel temperature) guarantee better dispersion, so increased contact between the individual nanotubes and matrix.

PC/ABS blends filled with carbon nanotubes are studied by Xiong et al.[3] and Sun et al.[4]. The migration or controlled location of MWCNT is reported. In both cases the approach of blend preparation by the researchers from the neat components is present. In addition, the affinity of carbon nanotubes to PC component at the defined PC-to-ABS ratio shows the challenges of achieving a uniform distribution of MWCNT in both components.

In this work, we present PC/ABS-MWCNT nanocomposites prepared by the dilution of predispersed masterbatch on twin-screw extruder at two processing temperatures. In this industrial approach, the nanocomposites are formed from the commercial blend. Such an attempt allows studying the behavior of multiphase materials at conditions different from the commonly reported.[3,4] Common method of prior carbon nanotubes introduction to one of the blend components is here changed to the direct addition of the nanofiller to form PC/ABS-MWCNT masterbatch. Complete material characterization is reports. The effects of SME applied to the material during processing show the influence of process parameters. Morphology of the nanocomposites is characterized by light-transmission microscopy (LTM), scanning electron microscopy (SEM), and Raman spectroscopy. Thermal properties are investigated by thermogravimetric analyses (TGA) and differential scanning calorimetry (DSC) while mechanical properties are explored with dynamic-mechanical analysis (DMA) and tensile testing. Moreover, theoretical predictions of mechanical improvement are correlated with the experimental data.

EXPERIMENTAL

Commercial blend of PC and acrylonitrile-butadiene-styrene (PC/ABS) Bayblend® T85 was supplied by Bayer Material Science; contained 85 wt % of PC. The melt-volume flow rate was 12 cm^3/10 min and the Vicat softening temperature was 129°C (data provided by supplier). The multiwalled carbon nanotubes (MWCNT) NC7000 were supplied by Nanocyl. The average diameter was 9.5 nm and the average length was 1.5 μm (data provided by supplier).

The nanocomposites were obtained with a throughput of 1 kg h^{-1} on the twin-screw corotating laboratory extruder Prism Eurolab 16 (Thermo Fisher Scientific) with a length-to-diameter ratio (L/D) of 25. The screw profile was designed using Ludovic software (Sciences Computers Consultants). Nanocomposites were produced at 260 or 280°C with a screw speed of 400 rpm. The carbon nanotubes were fed to the extruder with a pneumatic feeder (Brabender Technologies) together with PC/ABS pellets. The final nanocomposites were subsequently formed with a dilution of 5.0 wt % MWCNT masterbatch (prepared in the same conditions as dilution) to concentrations between 0.5 and 3.0 wt %. PC/ABS pellets and masterbatch pellets were dried in a vacuum at 100°C for 4 h before each processing stage. Rectangular samples with dimensions of 60 × 10 × 2 mm^3 (following modified standard ISO 127) were compression molded on a Collin 6300 hydraulic press at 260°C to be used in thermo-mechanical tests and for electrical conductivity measurements. Additionally, dog-bone specimens (following standard ISO 527-3) of the same condition were used in the evaluation of mechanical properties.

The morphology of the nanocomposites was studied by LTM on a Leica DMRX microscope and by SEM on a JEOL 7001F scanning electron microscope. Films 20–50 μm thick for LTM study were heat-pressed from pellets. SEM samples were platinum-coated using a Baltec SCMCS010 sputtering device. Raman spectroscopy measurements were done on a Horiba XploRA with 532 nm laser LCM-S-11 and CCD detector.

TGA was done on a Q5000 instrument (TA Instruments). Pellets weighting 10 mg were heated from 50 to 600°C at a heating rate of 20°C min^{-1} in a nitrogen atmosphere. DSC was done on a Diamond (Perkin-Elmer). Each sample was heated from 40 to 280°C at a heating rate of 10°C min^{-1} to erase the thermal history. This was followed by cooling to 40°C at the same rate and then a second heating to 280°C to determine the glass transition temperature and enthalpies.

The viscoelastic properties of nanocomposites were investigated on an AR G2 rotational rheometer (TA Instruments) with parallel plate geometry (diameter 25 mm) at 280°C. Strain was set to 1% according to the results of a strain sweep. A DMA was done on a DMA-2980 (TA Instruments) with the dual cantilever clamp at a vibration frequency of 1 Hz, a temperature range from 35 to 200°C and scan rate of 3°C min^{-1}. Tensile testing was performed according to ASTM D-638 on an Instron Universal Machine 3343 with 5 kN load cell and an extension velocity of 5 mm min^{-1}. The experiments were conducted with constant conditions: 50 ± 5% HR and 24 ± 2°C.

The electrical resistivity was measured by two-point contact configuration (following the ISO 3915 standard) on a Keithley 2000 Multimeter source/meter. Silver electrodes were painted on the samples to improve contact with the measuring electrodes.

RESULTS AND DISCUSSION

Morphology

The morphology of the nanocomposites obtained by melt-mixing an immiscible PC/ABS blend with carbon nanotubes is present on the LTM images in Figure 1. A relatively good dispersion of MWCNT with minor agglomeration was achieved for all applied processing conditions, showing little difference between the low and high temperatures of the barrels. Nanocomposites prepared at 260°C showed more homogeneous morphology than those produced at 280°C. This difference was clearer with higher MWCNT loads. Moreover, at 260°C, the reduction of the quantity of agglomerates per controlled area appeared, along with an increase of the size of the agglomerates as the nanofiller load changed from 1.0 to 3.0 wt %. Such agglomerate behavior can be correlated with the SME curves shown in Figure 2 and calculated with eq. (1). This important

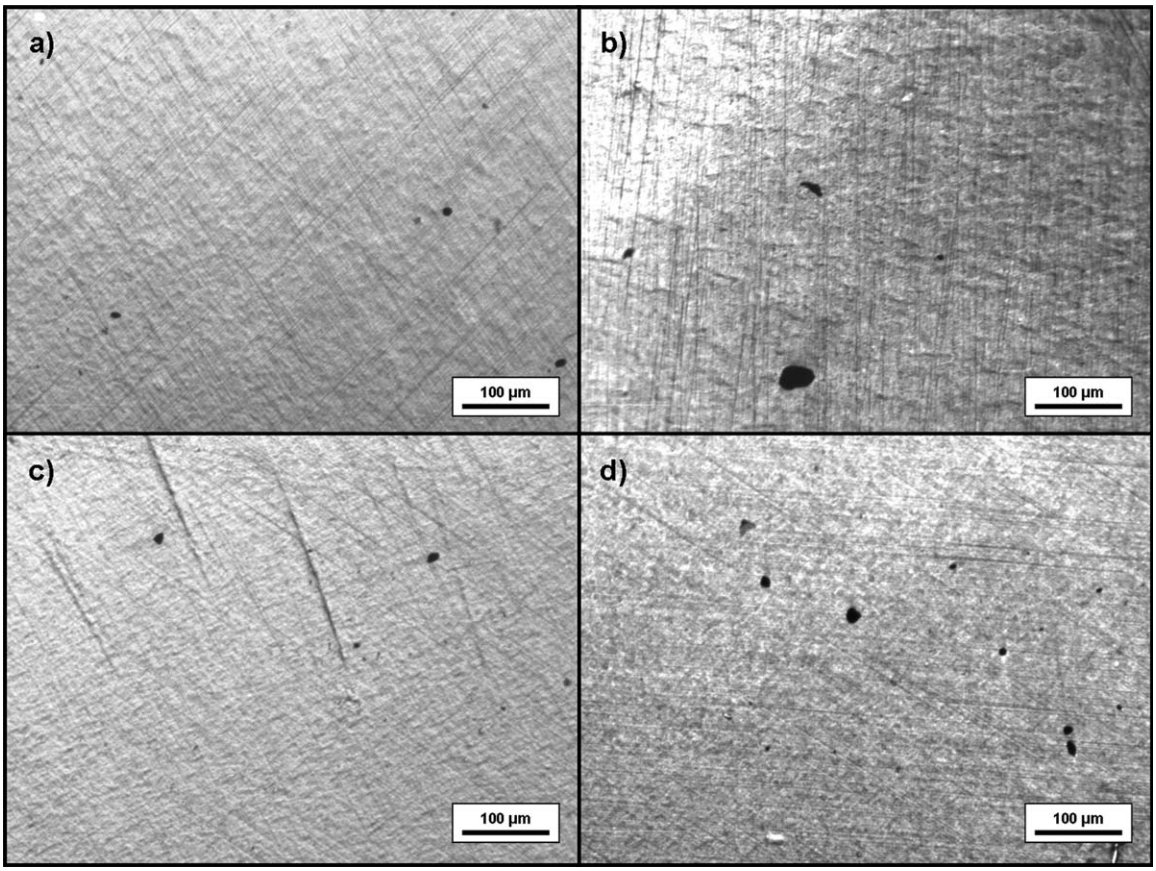

Figure 1. LTM images of PC/ABS-MWCNT nanocomposite processed at 260°C: (a) 1.0 wt %, (b) 3.0 wt %, and 280°C, (c) 1.0 wt %, and (d) 3.0 wt %.

parameter characterized by showing the effectiveness of the selected conditions with εP representing the effective power of the motor, τ representing the torque, and Q representing the throughput. The input data also contained a screw speed ratio between the applied (v_{proc}) and maximum (v_{max}) values. The throughput Q was constant for all experiments to facilitate equal analysis of the results. However, reports regarding the influence of that parameter exist in the literature.[11] Therefore, the SME was understood as a relation between various mutually correlated parameters and was directly proportional to torque (influenced by melt viscosity) and screw speed.[17] Clear dependence of SME on melt temperature and the MWCNT load is present in Figure 2. Higher values of shear applied at lower temperatures shows a clear increase of SME. This behavior can be derived from higher viscosity at lower temperatures as well as higher MWCNT loads. Sufficient mixing energy gives the possibility of obtaining a relatively good dispersion of carbon nanotubes.[11]

$$SME = \frac{\varepsilon P \cdot \tau \cdot \frac{v_{proc}}{v_{max}}}{Q} \quad (1)$$

$$E_{nc} = k_A \frac{1 + \zeta \eta V_{CNT}}{1 - \eta V_{CNT}} E_m \quad (2)$$

$$\eta = \frac{K_\omega \left(\alpha \frac{E_f}{E_m}\right) - 1}{K_\omega \left(\alpha \frac{E_f}{E_m}\right) - \zeta} \quad (3)$$

$$\zeta = \frac{2l}{d} \quad (4)$$

Previous reports on PC/ABS investigations provide definitions of the immiscible phases on the SEM micrographs.[18] The morphology of nanocomposites studied on the SEM micrographs shows the preferential locations of carbon nanotubes in the PC, appearing as a smooth surface, as opposed to ABS (Figure 3).

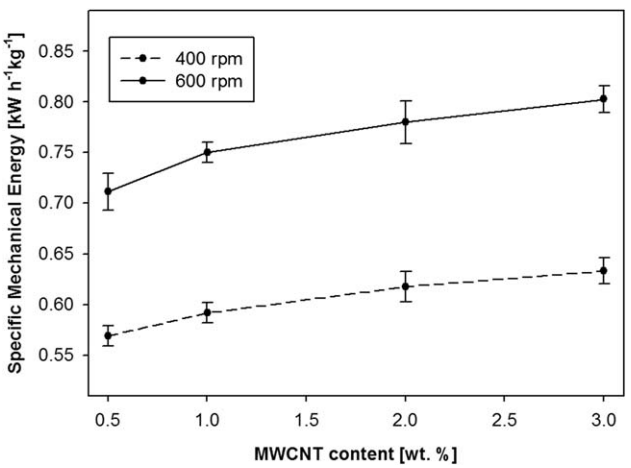

Figure 2. SME of PC/ABS-MWCNT nanocomposites extruded at various temperatures.

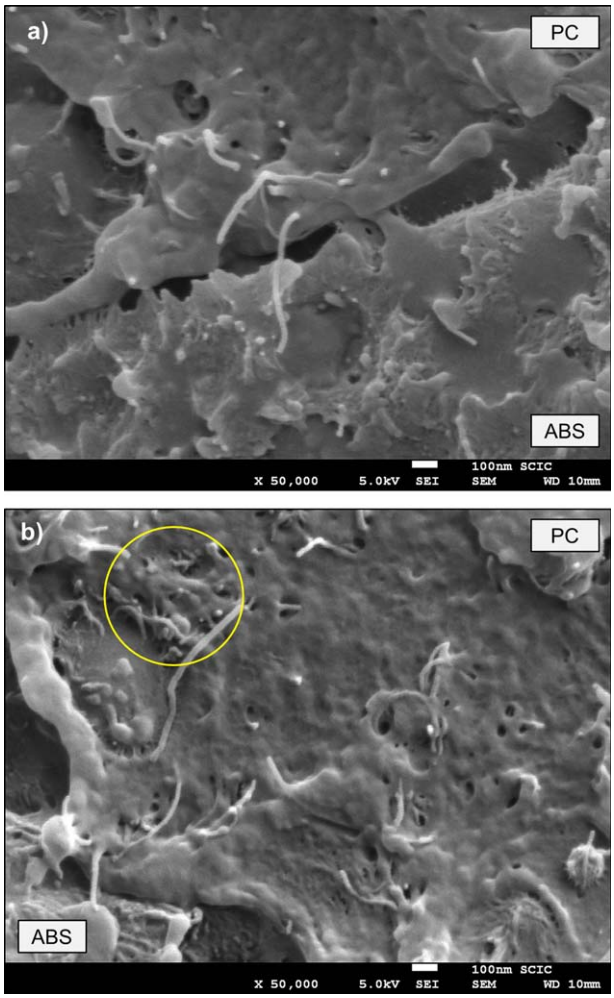

Figure 3. SEM micrographs of PC/ABS-MWCNT nanocomposite processed at 260°C: (a) 1.5 wt % and (b) 3.0 wt % with circled agglomerate. [Color figure can be viewed in the online issue, which is available at wileyonlinelibrary.com.]

This situation does not change with an increase of the MWCNT load or in various processing conditions. These conclusions can be correlated with the calculations of surface energies and wetting coefficient between the MWCNT and matrix components.[19,20] The interfacial tension obtained from partial surface tensions between the defined phases of the blend shows that carbon nanotubes have significantly higher affinity to PC, which agrees with the observations. Moreover, the agglomeration behavior expected at higher carbon nanotube loads was present in the SEM micrographs. Figure 3(b) shows entangled and individual MWCNT, while for lower nanofiller concentrations and mainly well-dispersed structures were present.

The vibrational spectra of PC/ABS present in Figure 4 shows the characteristic pattern between 600 and 2000 cm^{-1}. The Raman bands at 1880, 1112, and 885 cm^{-1} are representing carbon-hydrogen in-plane and out-of-plane wagging modes. Broad band between 1200 and 600 cm^{-1} are related to C—O stretching and C—H deformation.[21] The characteristic bands of pristine MWCNT appear at 1340 and 1575 cm^{-1} for D- and G-bands, respectively.[21] For nanocomposites, the bands were

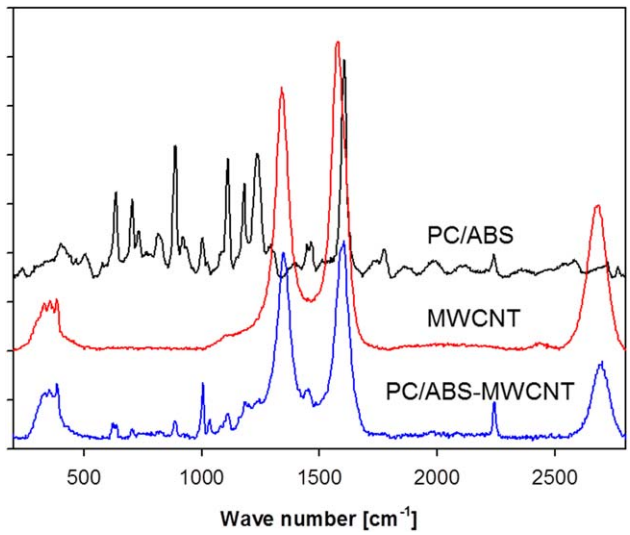

Figure 4. Raman spectra of PC/ABS, MWCNT and resulting nanocomposite (1.0 wt %). [Color figure can be viewed in the online issue, which is available at wileyonlinelibrary.com.]

shifted towards the higher wave-number (blue shift), showing the positions at about 1347 and 1599 cm^{-1} for D- and G-bands, respectively. This effect is explained as the result of MWCNT disentanglement and was reported in earlier studies.[22] The bands at about 1500 cm^{-1} that overlap with the G-band of the MWCNT, made the intensities ratio of characteristic bands (D/G) a more effective parameter. In this regard, the decrease of D/G was observed from 0.99 ± 0.01 for MWCNT and 0.95 ± 0.01 for PC/ABS with 1.0 wt % MWCNT. This can be related to the local stresses between MWCNT and the polymer,[23,24] represented by the mechanical compression transferred from the matrix to the MWCNT.[25]

Thermal Properties

Figure 5 shows the thermal degradation behavior of pristine PC/ABS as well as the selected nanocomposites measured by TGA. Both components of the matrix can be distinguished by

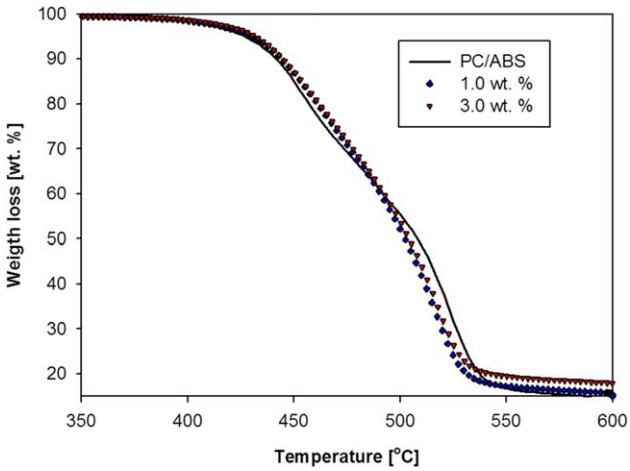

Figure 5. Thermal degradation curves for pristine matrix and two selected nanocomposites. [Color figure can be viewed in the online issue, which is available at wileyonlinelibrary.com.]

Table I. Thermal Properties of PC/ABS Nanocomposites Processed at 260°C

	ABS			PC		
MWCNT (wt %)	T_g[a] (°C)	ΔC_p[b] ($Jg^{-1}deg^{-1}$)	w.d.[c] (°C)	T_g[a] (°C)	ΔC_p[b] ($Jg^{-1}deg^{-1}$)	w.d.[c] (°C)
0.0	119.2	0.082	452.2	141.0	0.115	514.0
0.5	114.8	0.062	454.6	142.0	0.118	515.1
1.0	114.6	0.058	457.7	142.6	0.139	516.3
2.0	114.2	0.048	457.9	143.0	0.159	517.5
3.0	113.9	0.043	458.2	143.4	0.165	518.3

[a] Glass transition temperature.
[b] Change of heat capacity at glass transition.
[c] Peak maximum of weight derivative obtained by TGA.

two-step decomposition. Moreover, the initial part of the curve (c.a. 400–475°C) representing the degradation of ABS, showed a slight increase of the thermal stability after the incorporation of carbon nanotubes. Even though the PC seemed to show no significant change after the formation of the nanocomposite, the results present in Table I show a similar trend for both blend components. The thermal stability of PC decreased slightly, which was observed with an increase of the carbon nanotubes load from 1.0 to 3.0 wt %. Similar behavior was reported in earlier studies.[26] This was explained by the impurities in the nanofiller (e.g., metal ions) that can act as Lewis acids and weaken radicals causing easier thermal degradation.

Table I shows the DSC results: the glass transition temperature (T_g) and change of heat capacity at the glass transition temperature (ΔC_p) for investigated nanocomposites. The trend was opposite for both PC/ABS phases. Chain mobility based on the interactions between well-dispersed individual carbon nanotubes and polymer chains can be investigated with the heat capacity.[27] The network of carbon nanotubes reduced the freedom degree of polymer chains, which caused the decrease of ΔC_p. This effect occurred during the ABS phase only with a reduced amount of MWCNT. However, with the increase of carbon nanotube load, a morphological evolution can occur, locating more nanofiller in ABS. This was described by Xiong et al.[3] as an effect related to the processing conditions. Nevertheless, this phenomenon can also be related to the increase of the content of the carbon nanotubes. Conversely, agglomeration in PC with an increased nanofiller load provided a higher mobility of polymer chains, which affected the change of the heat capacity at the glass transition temperature.

Rheology

The rheology of PC/ABS-MWCNT nanocomposites in Figure 6 shows a clear dependence on the carbon nanotubes load. An increase of storage modulus (G') with the increase of the MWCNT load and with frequency was observed. Solid-like behavior with a rubber plateau at low angular frequencies was more obvious at higher nanofiller loads and could be observed above defined molecular carbon nanotube-polymer chain entanglements.[7] The transition between liquid- and solid-like behavior was expected below 0.5 wt %[28] and was also related to the molecular weight of the polymer chains that were clearly reduced after processing. Such rheological percolation is believed to mark the significant increase of MWCNT network contribution (as it appears for electrical percolation threshold).[7] Before that point, at lower concentrations of MWCNT, nanotubes-polymer networks dominate. Disentanglement of tight microstructures of nanofiller network is more difficult than disentanglement of polymer-polymer or polymer-MWCNT networks at low frequencies. Therefore, substantial influence of the carbon nanotubes on the polymer relaxation dynamics explains the linear viscoelastic properties observed at low nanofiller loads and at low frequencies.[29] Besides, the change of modulus curve at 3.0 wt % MWCNT is nearly frequency-independent.

Mechanical Properties

Tan δ, defined as the ratio of loss modulus to storage modulus, is a measure of inherent material damping (energy dissipation). Figure 7 shows the value of the tan δ (maximum peak) according to the incorporation of the MWCNT into the PC/ABS matrix. An increase of tan δ with increase of the carbon nanotube load was observed for both matrix components. Nevertheless, the improvement was higher in the major phase (PC) than in the minor phase (ABS) an increase in the transition temperatures in both phases indicated the improvement of the mechanical properties. These observations can be correlated with these results, regarding tan δ as cross-linking sensitive parameter. Higher carbon nanotubes concentrations created more entanglements

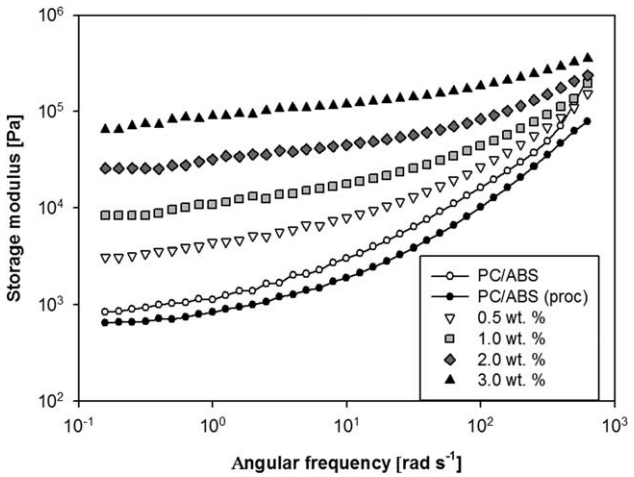

Figure 6. Storage modulus of the neat, the processed PC/ABS, and its selected nanocomposites with MWCNT.

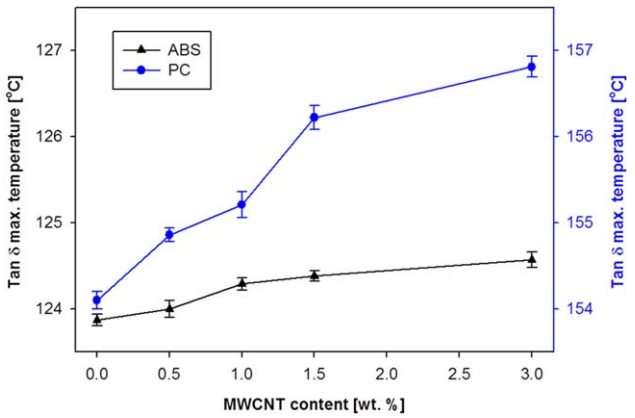

Figure 7. Dynamic mechanical analyses results for PC/ABS and its nanocomposites with MWCNT. [Color figure can be viewed in the online issue, which is available at wileyonlinelibrary.com.]

between polymer chains that can be understood as a formation of this network influencing the energy absorption.

The influence of the content of carbon nanotubes content on Young's modulus is shown in Figure 8. Significant improvement of the stiffness was achieved after the introduction of 0.5 wt % MWCNT. A further increase of nanofiller concentrations hardly changed Young's modulus. Nevertheless, Table II shows an increase of yield stress and a decrease of elongation at the break at higher carbon nanotube loads. This behavior was expected and was observed by other authors.[30] A different trend in Young's modulus below and above 0.5 wt % can be related to higher agglomeration at higher loads. In this regard, the change of the load transfer mechanism can explain the decrease of ductility at elevated carbon nanotube loads.

A comparison of the experimental data of PC/ABS nanocomposites with a theoretical model based on the Halpin-Tsai equations[31] is shown in Figure 8. Reported modifications of this method, originally related to microfillers, broadened its application range to nanocomposites.[32–34] The theoretical values of Young's modulus calculated with eq. (2) agreed with the experimental data in the entire MWCNT concentration range. Factor η described by eq. (3) defines the efficiency of the nanofiller while ζ, eq. (4) is related to the geometry and boundary conditions of the reinforcement of the individual nanotube. Young's modulus of nanofiller (E_f) and PC/ABS (E_m) are 980 and 1.2 GPa, respectively. The MWCNT load was defined by the volume fraction (V_f). However, a rather poor agreement between the theoretical and experimental data was achieved with the classic Halpin-Tsai model. Correct orientation factor α, experimental k_A factor and waviness coefficient K_ω need to be selected to improve this, especially with higher carbon nanotube loads. According to the literature, α value of 0.17 represents randomly oriented MWCNT, which was the situation expected in this study.[32] The waviness coefficient usually ranges between 0 and 1 and represents the share of force transferred by the MWCNT along the central axis. Even though a nonmodified calculation method does not fit the experimental data independently on the waviness coefficient, a nonmodified method seems to agree with nanocomposites below 0.5 wt % MWCNT when a higher share of the long axes of the nanotubes is considered ($K_\omega = 0.2$). However, correct experimental curves fitting with the theory occur when nonlinear dependence between the carbon nanotubes loads and mechanical performance is defined.

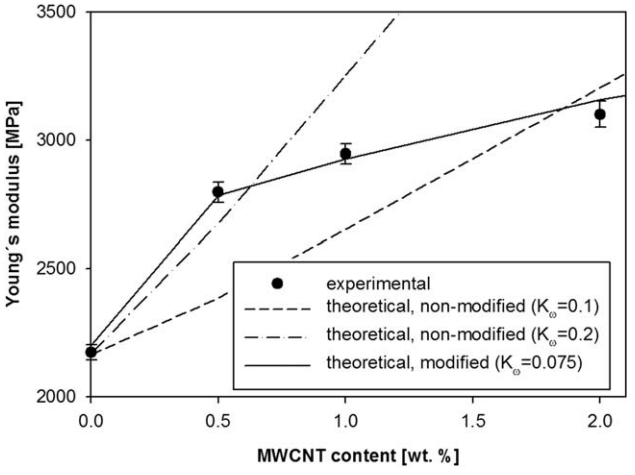

Figure 8. Young's modulus dependence on the MWCNT load in PC/ABS-MWCNT nanocomposites compared with theoretical data.

Table II. Mechanical Properties of PC/ABS Nanocomposites Processed at 260°C

	Mechanical properties		
MWCNT (wt %)	σ_y[a] (MPa)	ε_b[b] (%)	En[c] (J)
0.0	44.8 (±1.0)	10.0 (±0.1)	806.0 (±12)
0.5	52.5 (±1.1)	9.3 (±0.5)	628.5 (±29)
1.0	56.1 (±1.3)	8.7 (±0.5)	440.5 (±32)
2.0	56.6 (±1.2)	7.5 (±0.6)	381.2 (±30)
3.0	57.0 (±1.4)	6.3 (±0.8)	344.7 (±25)
5.0	57.9 (±1.3)	4.6 (±0.6)	260.0 (±32)

[a] Stress at yield point.
[b] Elongation at break.
[c] Elastic strain energy.

Electrical Properties

Figure 9 shows the electrical conductivity of nanocomposites obtained at various temperatures. The conductivity of neat PC/ABS, e^{-15} Scm^{-1}, was boosted about 14 orders of magnitude with the load of 1.0 wt % MWCNT. The rapid improvement of electrical properties with an increase of nanofiller content occurred above 2.0 wt % marking the percolation threshold. However, only minor differences were observed with the change of melt temperature (between 260 and 280°C). In both cases, the electrical percolation (Φ_e) was present in almost exactly equal concentrations. In addition, the mechanical percolation observed in the flow curves occurred at lower loads than where the conductive network was formed. This can be related to different characteristics of both networks, regarding the polymer chains-nanotubes network in the latter case.[7,28,29] The electrical conductivity demands direct nanotube-nanotube contact or very small distances to provide charge paths between the

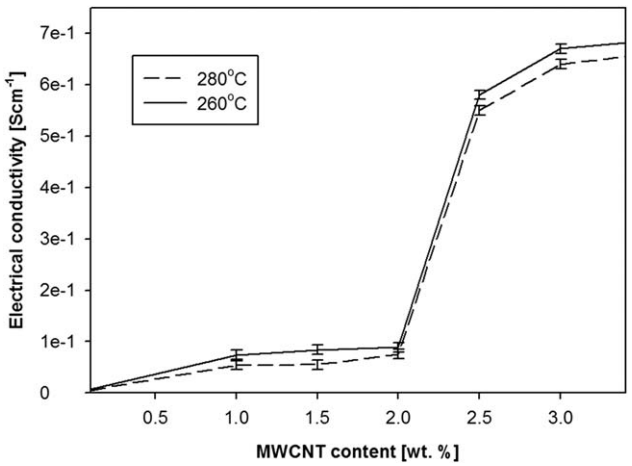

Figure 9. Electrical conductivity of PC/ABS-MWCNT nanocomposites processed at different barrels temperature.

electrodes. Furthermore, immiscible blends showed double percolation phenomenon based on the continuity of conductive filler-rich phases in the other phases of the matrix. Finally, electrical conductivity varied almost at an order of magnitude between 2.0 and 3.0 wt %, which is rather uncommon behavior after the percolation point.

CONCLUSIONS

In this work, we presented the results of the characterization of PC/ABS-MWCNT nanocomposites processed by melt-mixing. SME was found to show a clear difference, favoring lower processing temperatures. Commercial, immiscible blend forms nanocomposites with good morphologies with the majority of the nanofiller located in the PC. This agrees with the literature calculations based on the surface energies of blend components. The dilution of pre-dispersed masterbatches on twin-screw extruder resulted in the improvement of thermal-, mechanical- and electrical properties. The thermal properties were related to the dispersion of the MWCNT in the polymer matrix. The change of the heat capacity at the glass transition temperatures indicated the increase of carbon nanotube content in the ABS phase at elevated loads. In addition, the mechanical percolation estimated on the storage modulus (G') curves appeared to be significantly lower than electrical percolation, indicating a difficult-to-achieve conductive path in commercial PC/ABS as well as the presence of a MWCNT-rich phase. The fact that the mechanical properties improved with an increase of the MWCNT load correlated with the theoretical values calculated with the modified Halpin-Tsai method.

A balance between the mechanical and electrical properties observed during this investigation creates an attractive opportunity for the automotive and electronic industries. The applicability of these nanocomposites by injection molding of PC/ABS-MWCNT nanocomposites will be presented in a future study.

ACKNOWLEDGMENTS

This work is funded by the European Community's Seventh Framework Program (FP7-PEOPLE-ITN-2008) within the CONTACT project Marie Curie Fellowship under grant number 238363.

REFERENCES

1. Göldel, A.; Pötschke, P. In Polymer-Carbon Nanotube Composites; McNally, T., Pötschke, P., Eds.; Woodhead Publishing: Oxford, **2011**; Vol. *1*, Chapter 19, pp 587.
2. Sathyanarayana, S.; Wegrzyn, M.; Olowojoba, G.; Benedito, A.; Gimenez, E.; Hübner, C.; Henning, F. *Express Polym. Lett.* **2013**, *7*, 621.
3. Xiong, Z. Y.; Wang, L.; Sun, Y.; Guo, Z. X.; Jian, Y. *Polymer* **2013**, *54*, 447.
4. Sun, Y.; Gou, Z. X.; Yu, J. *Macromol. Mater. Eng.* **2010**, *295*, 263.
5. Yang, L.; Liu, F.; Xia, H.; Qian, X.; Shen, K.; Zhang, J. *Carbon* **2011**, *49*, 3274.
6. Pötschke, P.; Dudkin, S. M.; Alig, I. *Polymer* **2003**, *44*, 5023.
7. Pötschke, P.; Abdel-Goad, M.; Alig, I.; Dudkin, S.; Lellinger, D. *Polymer* **2004**, *45*, 8863.
8. Villmow, T.; Kretzschmar, B.; Pötschke, P. *Comp. Sci. Technol.* **2010**, *70*, 2045.
9. Villmow, T.; Pegel, S.; Pötschke, P.; Wagenknecht, U. *Comp. Sci. Technol.* **2008**, *68*, 777.
10. Duong, H. M.; Tamamoto, N.; Bui, K.; Papavassiliou, D. V.; Maruyama, S.; Wardle, B. L. *J. Phys. Chem. C* **2010**, *114*, 8851.
11. Sathyanarayana, S.; Olowojoba, G.; Weiss, P.; Calgar, B.; Pataki, B.; Mikonsaari, I.; Huebner, C.; Hening, F. *Macromol. Mater. Eng.* **2013**, *298*, 89.
12. Vega, J. F.; Martinez-Salazar, J.; Trujillo, M.; Arnal, M. L.; Müller, A. J.; Bredeau, S.; Dubois, P. *Macromolecules* **2009**, *42*, 4719.
13. Alig, I.; Lellinger, D.; Dudkin, S.; Pötschke, P. *Polymer* **2007**, *49*, 1020.
14. Hill, D. E.; Lin, Y.; Rao, A. M.; Allard, L. F.; Sun, Y. P. *Macromolecules* **2002**, *35*, 9466.
15. Alig, I.; Lellinger, D.; Engel, E.; Skipa, T.; Pötschke, P. *Polymer* **2008**, *49*, 1902.
16. Krause, B.; Villmow, T.; Boldt, R.; Mende, M.; Petzold, G.; Pötschke, P. *Comp. Sci. Technol.* **2011**, *71*, 1145.
17. Krause, B.; Pötschke, P.; Häußler, L. *Comp. Sci. Technol.* **2009**, *69*, 1505.
18. Krache, R.; Debbah, I. *Mater. Sci. Appl.* **2011**, *2*, 404.
19. Nuriel, S.; Liu, L.; Barber, A. H.; Wagner, H. D. *Chem. Phys. Lett.* **2005**, *404*, 263.
20. Barber, A. H.; Cohen, S. R.; Wagner, H. D. *Phys. Rev. Lett.* **2004**, *92*, 186103.
21. Ahmed, S. F.; Ji, J. W.; Moon, M. W.; Jang, Y. J.; Park, B. H.; Lee, S. H. *Plasma Process. Polym.* **2009**, *6*, 860.
22. Bokobza, L.; Zhang, J. *Express Polym. Lett.* **2012**, *6*, 601.
23. Deng, L.; Eichhorn, S. J.; Kao, C. C.; Young, R. *J. ACS Appl. Mater. Inter.* **2011**, *3*, 433.

24. Cooper, C. A.; Young, R. J.; Halsall, M. *Compos. A* **2001**, *32*, 401.

25. Yan, X.; Itoh, Y.; Kitahama, Y.; Suzuki, T.; Sato, H.; Miyake, T.; Ozaki, Y. *J. Phys. Chem. C* **2012**, *116*, 17897.

26. Schartel, B.; Braun, U.; Knoll, U.; Bartholmai, M.; Goering, H.; Neubert, D.; Pötschke, P. *Polym. Eng. Sci.* **2008**, *48*, 149.

27. Su, S. P.; Xu, Y. H.; Wilkie, C. A. In Polymer-carbon nanotube composites; McNally, T., Pötschke, P., Eds.; Woodhead Publishing: Oxford, **2011**, Vol. *1*, Chapter 16, pp 482.

28. Abdel-Goad, M.; Pötschke, P. *J. Non-Newton. Fluid.* **2005**, *128*, 2.

29. Du, F.; Scogna, R. C.; Zhou, W.; Brand, S.; Fischer, J. E.; Winey, K. I. *Macromolecules* **2004**, *37*, 9048.

30. Abbasi, S.; Carreau, P. J.; Derdouri, A. *Polymer* **2010**, *51*, 922.

31. Halpin, J. C.; Kardos, J. L. *Polym. Eng. Sci.* **1976**, *16*, 344.

32. Arasteh, R.; Omidi, M.; Rousta, A. H. A.; Kazerooni, H. *J. Macromol. Sci. Pure Appl. Chem.* **2011**, *50*, 2464.

33. Srivastava, V. K.; Singh, S. *Int. J.Compos. Mater.* **2012**, *2*, 2.

34. Jiang, Z.; Hornsby, P.; McCool, R.; Murphy, A. *J. Appl. Polym. Sci.* **2012**, *123*, 2676.